Experimental Study on Secondary Breakup of Droplets at Low Density Ratios

Surya Prakash R.*[1, 2], Prasad Boggavarapu[2], Ravikrishna R. V.[2]

[1]Department of Mechanical Engineering, Indian Institute of Technology, Dharwad, India
[2]Department of Mechanical Engineering, Indian Institute of Science, Bangalore, India
*Corresponding author email: surya@iitdh.ac.in

Abstract

Secondary breakup of droplets has been extensively studied to understand the mechanism of disintegration of droplets subjected to aerodynamic forces. Most of the experimental studies involve density ratios ($R = \rho_{liq} / \rho_{gas}$) greater than 500. However, the practical engine sprays encounter $R < 100$. On the other hand, some of the numerical investigations are carried out at $R < 50$. Thus, the current study aims to conduct single drop breakup experiments at density ratios < 500 to fill gaps in the literature. The experiments are performed in a high-pressure chamber (≤ 10 bar) with optical access which houses both the mono-disperse drop generator and a contoured nozzle to produce the required air jet. Elevating the chamber pressure to 10 bar results in lower R (up to ~75) and the aerodynamic Weber number (We) is varied by controlling the air jet velocity. Two different liquids and drop sizes are employed to verify the veracity of the observed results. It is observed that a lower density ratio causes the critical Weber number to have a slightly lower magnitude ($We \sim 9.4$) resulting in earlier disintegration of droplets. All the breakup regimes observed at atmospheric pressure are also observed at lower density ratios. A new breakup structure is observed to occur intermittently along with bag and bag-stamen breakup modes in the form of 'reverse-hat'. As the density ratio reduces the mode-changeovers are observed to occur at lower Weber numbers. On a log-log graph of density ratio vs. Weber number, the reduction in mode-changeover Weber number reduces almost linearly. The present study has thrown more light on the effect of low density ratios on secondary breakup, parts of which have been grey areas in the existing literature.

Keywords

Secondary breakup, density ratio, breakup regimes, atomization, high-pressure.

Introduction

When a drop is accelerated in a gas flow, it deforms due to the aerodynamic forces and eventually fragments into smaller droplets; this is termed as secondary breakup. Complete understanding of the breakup phenomenon is essential for an accurate determination of the drop size distribution which dictates the surface to volume ratio and hence the efficiency of drying, chemical reaction and combustion. Further, a better understanding of the breakup also helps in developing accurate multi-phase computational fluid dynamic models for sprays.

Both, numerous experimental and numerical studies have been performed to study secondary breakup of a droplets. Several articles [1]–[3] have periodically reviewed the advances in this field. The secondary breakup of a drop can be broadly categorised into six modes of deformation and breakup, primarily based on the aerodynamic Weber number and liquid Ohnesorge number: Vibrational mode [1], [4], Bag mode [5], [6], Bag and Stamen [1] and bag with multiple lobes. This phenomenon is thought to be due to Rayleigh-Taylor (RT) instability [6]–[8] or a combined RT/aerodynamic drag mechanism [2]. Sheet thinning mode of breakup is observed for further higher Weber numbers. Earlier, shear stripping (a viscous phenomenon) was assumed to be the mechanism , but later Liu & Reitz [9] proposed the sheet thinning mechanism, pointing out that it is an inviscid phenomenon. At further higher Weber

numbers Catastrophic mode of breakup is observed [10]. The transition of this breakup mode, as a function of Weber number, occurs very gradually. Different authors have proposed different transitional values of *We* (subject to the inaccuracies in the exact calculation of We and also the presence of impurities that alter the properties of the fluid used in the experiments (as shown in Table 1) and hence the reliability of the transitional values of *We* has remained a moot point. Other parameters that influence the breakup mechanism are density ratio, gas Reynolds number and liquid Ohnesorge number.

Several experimental studies have been performed in the past decades to understand the physics of secondary breakup [2]. Some of the studies have been performed at low density ratio (in the range 1 - 10) while most of the studies have been performed for water-air systems. Simpkins & Bales [11] and Harper et al. [12] presented experimental and theoretical studies, respectively, of secondary breakup of droplets at high Bond numbers. Patel & Theofanous [13] studied the fragmentation of drops moving at high speed for mercury/water system (density ratio ~ 10). Later, Theofanous et al. [7] studied droplet breakup at different static pressures over a wide range of gas densities, all in the rarefied range. Lee & Reitz [14] performed experiments for a range of gas densities (corresponding to density ratios 100 - 1000). They concluded that the Rayleigh number (and also the density ratio) have little effect on the drop breakup mechanisms, although the transition Weber numbers vary a bit. Gelfand [15] studied liquid(drop)-gas and dense liquid (drop)-light liquid systems and discussed the similarities between the features observed in the two systems. He noted that the value of the first critical Weber number in liquid-liquid systems is higher than the gas-liquid systems. Above studies indicate that the secondary breakup at lower density ratios may differ from higher density ratios. However, only limited amount of literature is available on secondary breakup at lower density ratios. Motivated by this, secondary breakup of droplets is studied at density ratios of around 75 by using a high-pressure chamber with optical access with an objective to improve the understanding the effect of density ration on the phenomenon.

Table 1 - Various modes of secondary breakup classified w.r.t. Weber number

Breakup Regime	Pilch and Erdman (1987)	Guildenbecher et al. (2009)	In-house Experiments
No breakup	We < 12	We < 11	We < 10
Bag	12 < We < 50	11 < We < 35	10 < We < 18
Bag-stamen	50 < We < 100	35 < We < 80	20 < We < 28
Dual-bag			30 < We < 46
Multi-bag			48 < We < 80
Shear		80 < We < 350	82 < We < 350

Experimental Setup

In the present study, aerodynamic breakup of droplets is studied by subjecting droplets generated from a mono-disperse droplet generator to an air jet exiting from a contoured nozzle. A schematic of the experimental setup is shown in Fig. 1. The experimental setup primarily consists of a pressure chamber which houses the air nozzle and the mono-disperse droplet generator. Compressed air from an air reservoir is sent through a mass flow controller to the contoured air-nozzle mounted on the left wall of the chamber which opens inside the chamber as shown in the figure. The outgoing flow from the chamber is sent through a needle valve. The pressure inside the chamber is adjusted and maintained at the required level (1,3, 5 or 10 bar) by controlling the incoming air-flow rate and choking the outgoing flow until the required pressure is built up in the chamber.

Internal section of the contoured nozzle with an exit diameter of 4 mm is designed so as to obtain a top-hat velocity profile at the exit which has been verified with the aid of PIV measurements. Different flow velocities at the exit of the nozzle are achieved by setting

different mass flow rates in the mass flow controller, thus varying the Weber number. The Weber number is defined based on the relative velocity between the liquid drop and the gas stream at t = 0, $We = \rho_g U_0^2 D_0 / \sigma$, where ρ_g is the density of the gas, U_0 is the relative velocity between droplet and gas jet, D_0 is the diameter of the droplet before deformation and σ is the surface tension between the liquid-air interface.
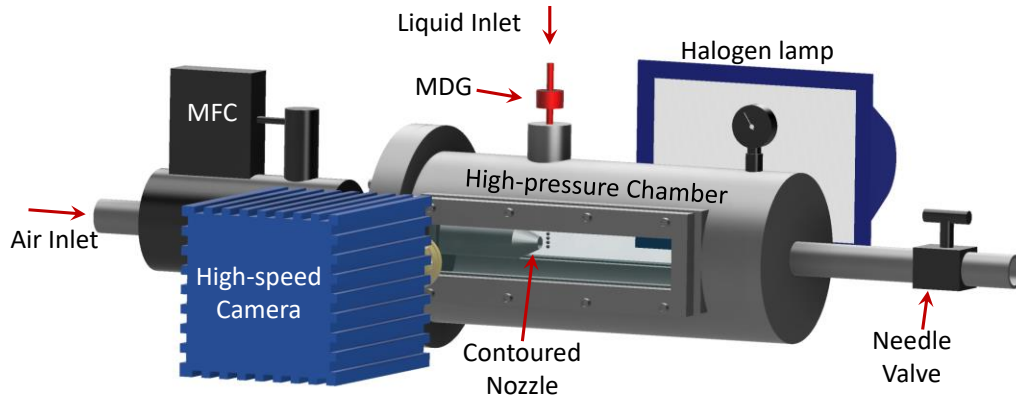
Figure 1. Experimental setup (MDG – Mono-disperse Droplet Generator, MFC – Mass Flow Controller)

A stream of mono-disperse drops is generated using a mono-disperse droplet generator mounted with its axis perpendicular to the axis of the air nozzle so that the droplets enter the air jet along the radial direction. Orifices of diameter 50 μm, 100 μm and 200 μm are used to generate droplets of diameters 100 μm, 200 μm and 400 μm respectively. The flow rate and the forcing frequency of the droplet generator can be varied to generate drops with different velocities but having the same diameter. As the air flow velocity is increased (for increasing We), the vertically falling droplet requires higher velocity to penetrate into the core of the air jet before undergoing breakup

Images are captured through the optical windows provided on the high-pressure chamber. A high-speed camera is used to record images at 50,000 fps with an exposure time of 1 μs. A high-intensity halogen lamp is used as the backlighting source to record shadow images of droplet breakup phenomenon. These images shall aid in determining the regime of drop breakup.

Experimental Setup

The experiments are performed to study the secondary breakup of two liquids, water and n-dodecane. The experiments at atmospheric pressure (1 bar) are performed in open atmosphere outside the chamber. The density ratios for water are 86 at 10 bar and density ratios for dodecane are 641, 214, 128 and 64 at 1 bar, 3 bar, 5 bar and 10 bar chamber pressure respectively. Table 2 shows the remaining experimental parameters. Two different orifices sizes of 200 μm and 50 μm are used for Water and Dodecane respectively to produce 400 μm water droplets and 100 μm Dodecane droplets. Choice of two different liquids and two different droplet diameters ensures that the results are independent of choice of liquid or droplet size. As mentioned previously, droplet diameters of 200 μm is used for studying dodecane droplet breakup at atmospheric pressure. It is observed during the course of experiments that sustaining a stream of intact mono-disperse drops is indeed a challenging task at higher gas pressures. The droplets were observed to breakup before entering the air jet when 200 μm orifice was used for n-Dodecane (because of low surface tension) which is another reason for the use of 50 μm orifice for n-Dodecane. Extra efforts were required to narrow down the operating conditions of the mono-disperse drop generator to produce well-

behaved droplet streams. Nevertheless, it was possible to achieve this across the entire Weber number range starting from 10 up to 100, spanning all the breakup regimes.

Table 2 - Range of parameters used in the present experiments

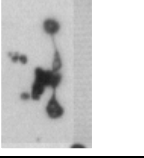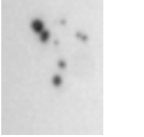| Parameter	Values	
Chamber Pressure	1, 3, 5 and 10 bar	
Density of ambient air (ρ_g)	1.17, 3.5, 5.85 and 11.69 kg/m^3	
Weber numbers (We)	10 - 100	
Liquids	**Water**	**Dodecane**
Density (kg/m^3)	1000	750
Viscosity (mPa.s)	0.8	1.34
Surface tension (mN/m)	72	26
Initial droplet sizes (μm)	400	100, 200
Density ratio (R)	**86**	**641, 214, 128 & 68**

Results and Discussion
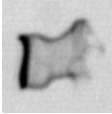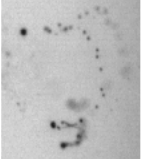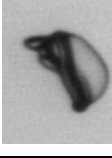
During the experiments, Weber number is varied by varying the air jet velocity, while maintaining the droplet sizes issued out from the mono-disperse drop generator at a constant value. Weber number is gradually increased, and the resultant drop breakup structures are scrutinised to detect the regime of breakup they are undergoing. The exercise is continued till the point where shear-thinning breakup of drops is clearly observed. As described in previous sections, high-speed shadowgraphy is used for recording images of droplet breakup phenomenon. In the following sections, a description of droplet breakup in each regime are described for water and dodecane droplets at 10 bar chamber pressure in comparison to breakup of droplet in similar regimes at atmospheric pressure. The images of droplet breakup at 3 bar and 5 bar are not shown because the phenomenon is similar to that of 10 bar. Later, a complete map of breakup regimes at various density ratios is presented.
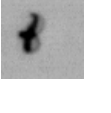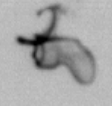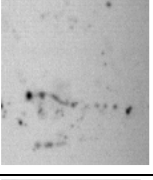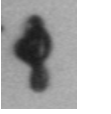
Bag breakup regime
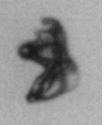
In bag breakup regime, the droplet first flattens into a disk-like structure as it encounters the air jet. Later, a rim forms at the periphery of the disk and a thinner diaphragm in the middle part. The diaphragm that is held by the rim is pushed by the dynamic pressure of the stagnating air flow to form a bag-like structure in the same direction of air flow. The rim also forms nodal structures with varying between 2-4 in number. Fig. 2 shows a sequence of high-speed images exhibiting this behaviour. At this stage it may be qualitatively stated that the bags formed at lower density ratios are of smaller size when compared those observed at atmospheric conditions. At atmosph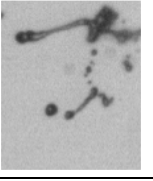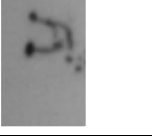eric pressure, the bag and rim are observed to elongate more before breakup compared to the breakup at 10 bar pressure. The number of nodes formed on the ring also show some variation at low density ratios, where they show a relatively consistent behaviour at atmospheric conditions. At 10 bar ambient pressure, this regime is observed to occur between Weber numbers of ~9.4 to ~13.2 as compared to the Weber number range of 10 to 18 at atmospheric pressure which indicates slight advancement of bag breakup regime.

Bag-stamen breakup regime

The flattened disc-like structures undergoes a change in subsequent deformation and expands to form a bag along with a stamen attached at the centre, protruding in the opposite direction of the air-jet, inside the bag. This process may be observed in Fig. 3 showing a high-speed sequence. Bag-stamen regime is observed between Weber numbers of ~16 to ~21 at 10 bar ambient pressures which is slightly ahead of the Weber number range of 20 to 28 at atmospheric pressure. Even in this regime, the deformation of film before rupture is observed to reduce at higher chamber pressures.

	Initial deformation	Intermediate stage	Final Stage
Chamber pressure = 1 bar Liquid = Dodecane Droplet size = 200 µm			
Chamber pressure = 10 bar Liquid = Water Droplet size = 400 µm			
Chamber pressure = 10 bar Liquid = Dodecane Droplet size = 100 µm			

Figure 2. Bag breakup regime at different chamber pressures

	Initial deformation	Intermediate stage	Final breakup
Chamber pressure = 1 bar Liquid = Dodecane Droplet size = 200 µm			
Chamber pressure = 10 bar Liquid = Water Droplet size = 400 µm			
Chamber pressure = 10 bar Liquid = Dodecane Droplet size = 100 µm			

Figure 3. Bag and stamen breakup regime at different chamber pressures

Reverse hat regime

At higher chamber pressures, around the Weber numbers ranging between 16 and 21 (overlapping with the bag and stamen breakup regime), a new phenomenon is observe which is not observed at atmospheric pressures. As mentioned before the flattening of liquid drop to form a flattened disc-like structure remains same. However, subsequently this flattened disc does not manifest into any previously known structures. Rather, it forms a hat-like structure with its convex portion faced towards the air-jet and hence termed as the 'reverse-hat' structure. The sequence of droplet breakup in this process is demonstrated in Fig. 4. There are no indicators to the usual rim-diaphragm formation during this process. Therefore, the reverse-hat like structure apparently seems to comprise of uniform sheet thickness and understandably does not form a bag-like structure. This reverse-hat structure collapses back into a lump at later stages and does not disintegrate considerably. This mode of breakup occurs intermittently along with bag-stamen breakup and occasionally with bag breakup and it happens exclusive of those modes, i.e. when the 'reverse-hat' forms there are no occurrences of bag or bag-stamen.

Dual-bag breakup regime

As the Weber number is increased further a dual-bag mode of breakup is observed. In this regime of breakup, formation and breakup of two bags is observed sequentially separated in time as shown in Fig. 5. Similar to the observations in bag breakup and bag and stamen breakup regimes, the growth of bag before rupture is significantly reduced as the ambient pressure increases. This regime is observe in the Weber number range of ~22 to ~32 at 10 bar pressure as compared to the Weber number range of 30 to 46 at atmospheric pressure. Here, it can be clearly seen that the critical Weber numbers separating different breakup regimes have advanced at higher chamber pressures.

	Initial deformation	Intermediate stage	Final breakup
Chamber pressure = 10 bar Liquid = Water Droplet size = 400 µm			
Chamber pressure = 10 bar Liquid = Dodecane Droplet size = 100 µm			

Figure 4. Reverse-hat regime observed at low density ratios

	Initial deformation	First bag formation	First bag breakup	Second bag formation	Second bag breakup
Chamber pressure = 1 bar Liquid = Dodecane Droplet size = 200 µm					
Chamber pressure = 10 bar Liquid = Water Droplet size = 400 µm					
Chamber pressure = 10 bar Liquid = Dodecane Droplet size = 100 µm					

Figure 5. Dual-bag breakup regime at different chamber pressures

Multi-bag breakup regime

At a range of higher Weber numbers (~35 to ~66) the droplets exhibit multi-bag mode of breakup. The diaphragm of liquid deforms to form multiple bags attached by thicker rib-like structure of the liquid. This may be observed in Fig. 6 showing a high-speed sequence. Lesser stretching of bag before rupture is observed at higher chamber pressures. This regime is observed between Weber numbers of 48 to 80 at atmospheric pressure experiments.

Shear breakup regime

The magnitude of Weber numbers is increased further (We > 60 at 10 bar), where the shear mode of breakup is exhibited. The velocities of the air stream are large enough to start stripping off of droplets from the edges of the flattened disc-like structure. Since this mode of breakup is not known to involve any complex structures, it seems to be very similar to the breakup witnessed at atmospheric conditions. Thus, the occurrence of various regimes is observed to advance as the chamber pressure is increased.

	Initial deformation	Intermediate stage	Final breakup
Chamber pressure = 1 bar Liquid = Dodecane Droplet size = 200 µm			
Chamber pressure = 10 bar Liquid = Water Droplet size = 400 µm			
Chamber pressure = 10 bar Liquid = Dodecane Droplet size = 100 µm			

Figure 6. Multi-bag breakup regime at different chamber pressures

Regime map

Figure 7 shows the complete set of experimental data from the present study which includes dodecane droplet breakup at 1, 3, 5 and 10 bar chamber pressures and water droplet breakup at 10 bar chamber pressure. Both the axes of the graph are represented in $\log_{10}$ scale to reduce cluttering of data towards lower weber numbers and lower density ratios. The experimental points which correspond to one regime of breakup are represented in a colour. The figure clearly shows that the minimum Weber number when the droplets undergo bag breakup reduces at lower density ratios. Also, the changeover Weber numbers separating different regimes of breakup have advanced at lower density ratios compared to those of higher density ratios. The straight lines drawn between groups of same coloured experimental points approximately show the regime boundaries. Thus, on a log-log graph of density ratio Vs Weber number the changeover Weber numbers advance approximately linearly. As per the knowledge of the authors this trend is reported for the first time in the literature.
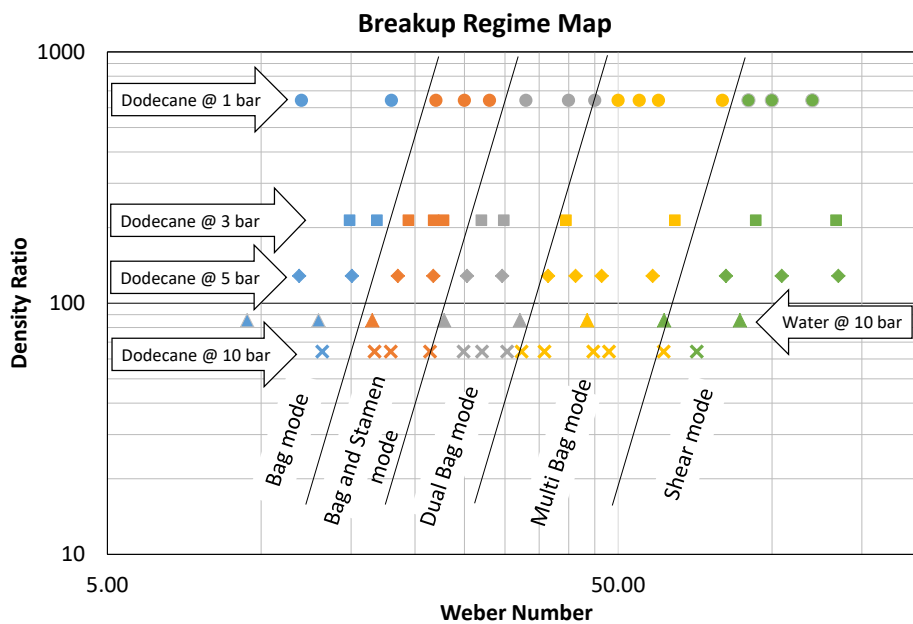

Figure 7. Secondary breakup regime map

Summary and Conclusions

Though secondary breakup has been extensively investigated in the past, there is still no clear understanding concerning the effect of density ratio (R), which is very relevant in practical applications such as gas turbine engines and IC engines. The current work addresses this gap and investigates the single droplet breakup at low density ratios with the help of a high-pressure chamber housing the mono-disperse drop generator and a contoured air nozzle. The lower density ratio is observed to slightly lower the critical Weber number (We~9.4) implying that the drops begin to disintegrate little earlier as compared to that at atmospheric pressure. Though all the well-known modes of breakup are observed, they are all witnessed at slightly lower Weber number ranges. The bag and bag-stamen breakup occur within a small range of Weber numbers immediately after crossing the critical Weber number, while the multi-bag breakup has an extended range. There is also a new breakup structure, 'Reverse-hat', occurring intermittently more often along with bag-stamen regime and less often with bag breakup. This phenomenon is not observed at atmospheric conditions. A detailed comparison of regime changeover Weber numbers with density ratios shows that the changeover of regimes occurs at lower weber numbers for lower density ratios. On a log-log graph of Density ratio vs. Weber number (R vs. We), the changeover Weber numbers reduce almost linearly with density ratio. Therefore, the present work is a clear pointer towards the difference in secondary breakup behaviour at low density ratio conditions.

References

[1] Pilch, M. and Erdman, C.A., 1987, International journal of multiphase flow, 13(6), pp.741-757.
[2] Guildenbecher, D.R., López-Rivera, C. and Sojka, P.E., 2009, Experiments in Fluids, 46(3), pp.371-402..
[3] Faeth, G.M., Hsiang, L.P. and Wu, P.K., 1995, International Journal of Multiphase Flow, 21, pp.99-127..
[4] Hsiang, L.P. and Faeth, G.M., 1992, International journal of multiphase flow, 18(5), pp.635-652.
[5] Chou, W.H. and Faeth, G.M., 1998, International journal of multiphase flow, 24(6), pp.889-912..
[6] Jain, M., Prakash, R.S., Tomar, G. and Ravikrishna, R.V., 2015, Proceedings of the Royal Society A: Mathematical, Physical and Engineering Sciences, 471(2177), p.20140930.
[7] Theofanous, T.G., Li, G.J. and Dinh, T.N., 2004, J. Fluids Eng., 126(4), pp.516-527.
[8] Zhao, H., Liu, H.F., Li, W.F. and Xu, J.L., 2010, Physics of Fluids, 22(11), p.114103.
[9] Liu, Z. and Reitz, R.D., 1997, International journal of multiphase flow, 23(4), pp.631-650.
[10] Liu, A.B. and Reitz, R.D., 1993, Atomization and sprays, 3(1).
[11] Simpkins, P.G. and Bales, E.L., 1972, Journal of Fluid Mechanics, 55(4), pp.629-639.
[12] Harper, E.Y., Grube, G.W. and Chang, I.D., 1972, Journal of Fluid Mechanics, 52(3), pp.565-591.
[13] Patel, P.D. and Theofanous, T.G., 1981 Journal of Fluid Mechanics, 103, pp.207-223.
[14] Lee, C.H. and Reitz, R.D., 2000, International Journal of Multiphase Flow, 26(2), pp.229-244.
[15] Gelfand, B.E., 1996, Progress in energy and combustion science, 22(3), pp.201-265.